

THE STAR FORMATION NEWSLETTER No. 344 (#1-6)

塚越崇(NAOJ)

3 Sep 2021

1. **A Circumplanetary Disk Around PDS70c**
2. **The Substructures in Disks undergoing Vertical Shear Instability: II.
Observational Predictions for the Dust Continuum**
3. Hourglass Magnetic Field from a Survey of Current Density Proles
4. The STAR-MELT Python package for emission line analysis of YSOs
5. Core mass function of a single giant molecular cloud complex with 10^4 cores
6. The GUAPPOS project II. A comprehensive study of peptide-like bond molecules

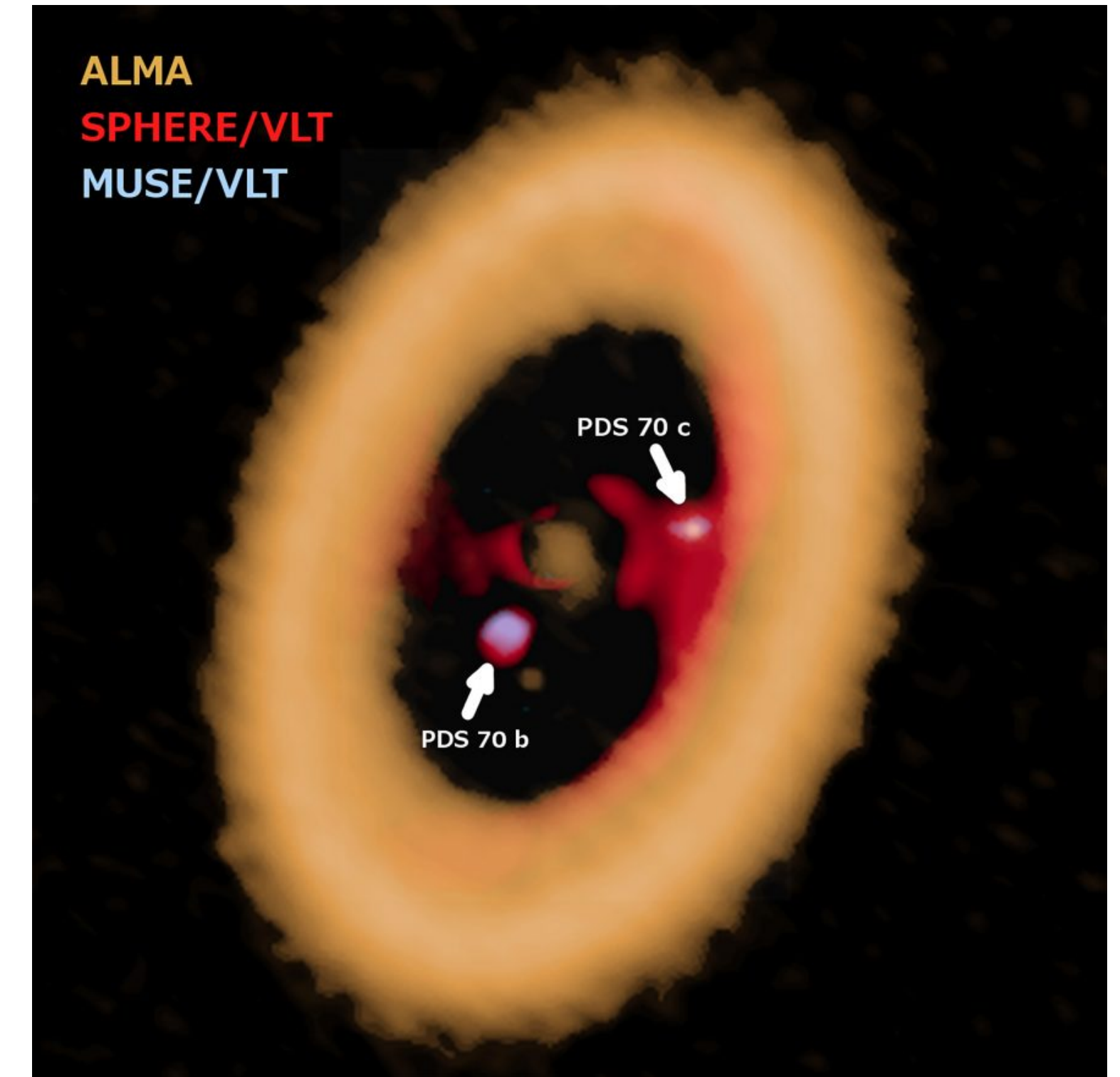
A Circumplanetary Disk Around PDS70 c

M.Benisty et al.

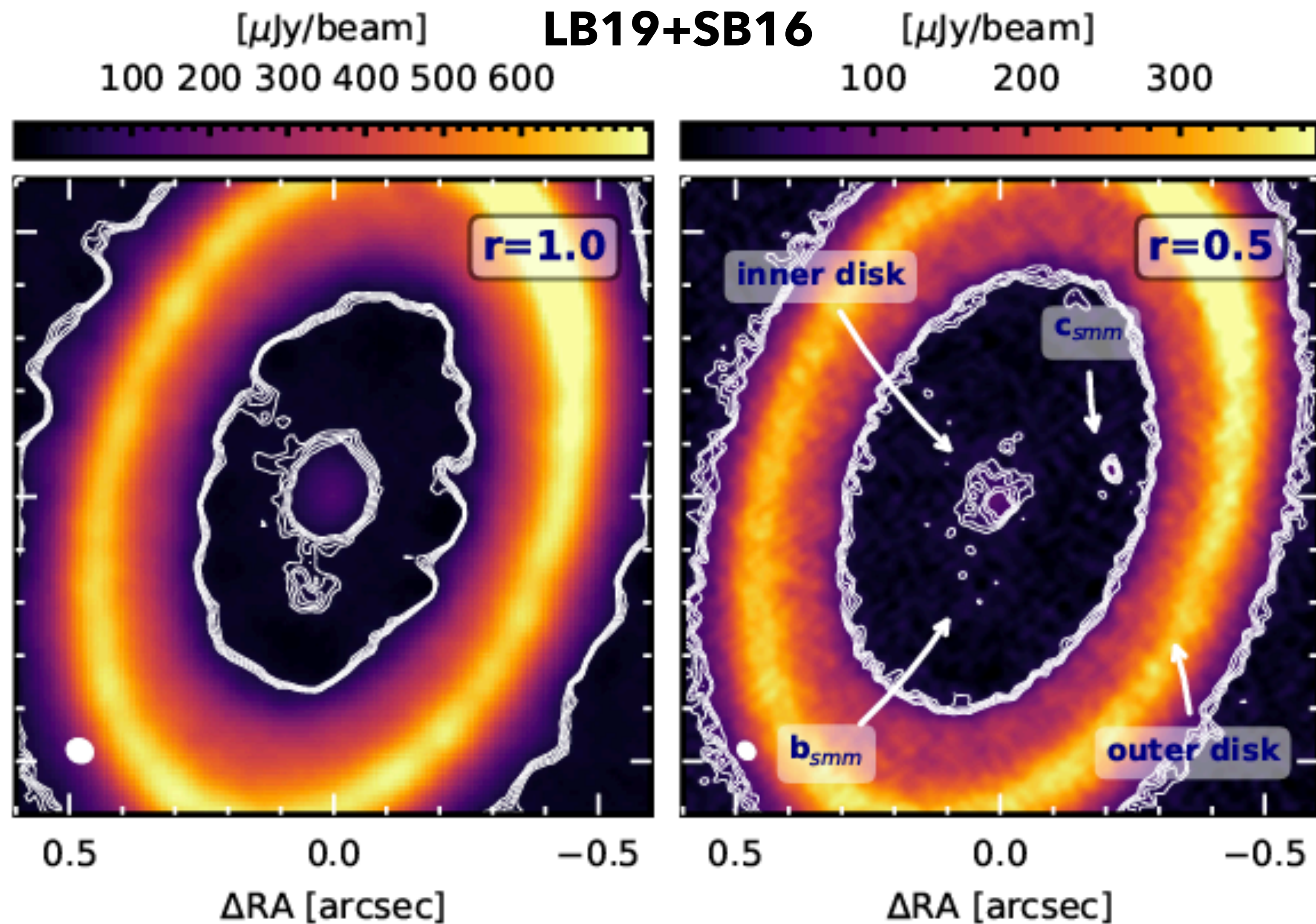
PDS 70 is a unique system in which two protoplanets, PDS 70 b and c, have been discovered within the dust-depleted cavity of their disk, at ~ 22 and 34 au respectively, by direct imaging at infrared wavelengths. Subsequent detection of the planets in the $H\alpha$ line indicates that they are still accreting material through circumplanetary disks. In this Letter, we present new Atacama Large Millimeter/submillimeter Array (ALMA) observations of the dust continuum emission at $855\,\mu\text{m}$ at high angular resolution (~ 20 mas, 2.3 au) that aim to resolve the circumplanetary disks and constrain their dust masses. Our observations confirm the presence of a compact source of emission co-located with PDS 70 c, spatially separated from the circumstellar disk and less extended than ~ 1.2 au in radius, a value close to the expected truncation radius of the circumplanetary disk at a third of the Hill radius. The emission around PDS 70 c has a peak intensity of $\sim 86 \pm 16\,\mu\text{Jy beam}^{-1}$ which corresponds to a dust mass of $\sim 0.031\,M_{\oplus}$ or $\sim 0.007\,M_{\oplus}$, assuming that it is only constituted of $1\,\mu\text{m}$ or $1\,\text{mm}$ sized grains, respectively. We also detect extended, low surface brightness continuum emission within the cavity near PDS 70 b. We observe an optically thin inner disk within 18 au of the star with an emission that could result from small micron-sized grains transported from the outer disk through the orbits of b and c. In addition, we find that the outer disk resolves into a narrow and bright ring with a faint inner shoulder.

- PDS70円盤に対してALMA高解像度観測を実行
 - 解像度 $\sim 1/3$ に改善
- 惑星候補と円盤を分離して検出 \rightarrow 物理量導出

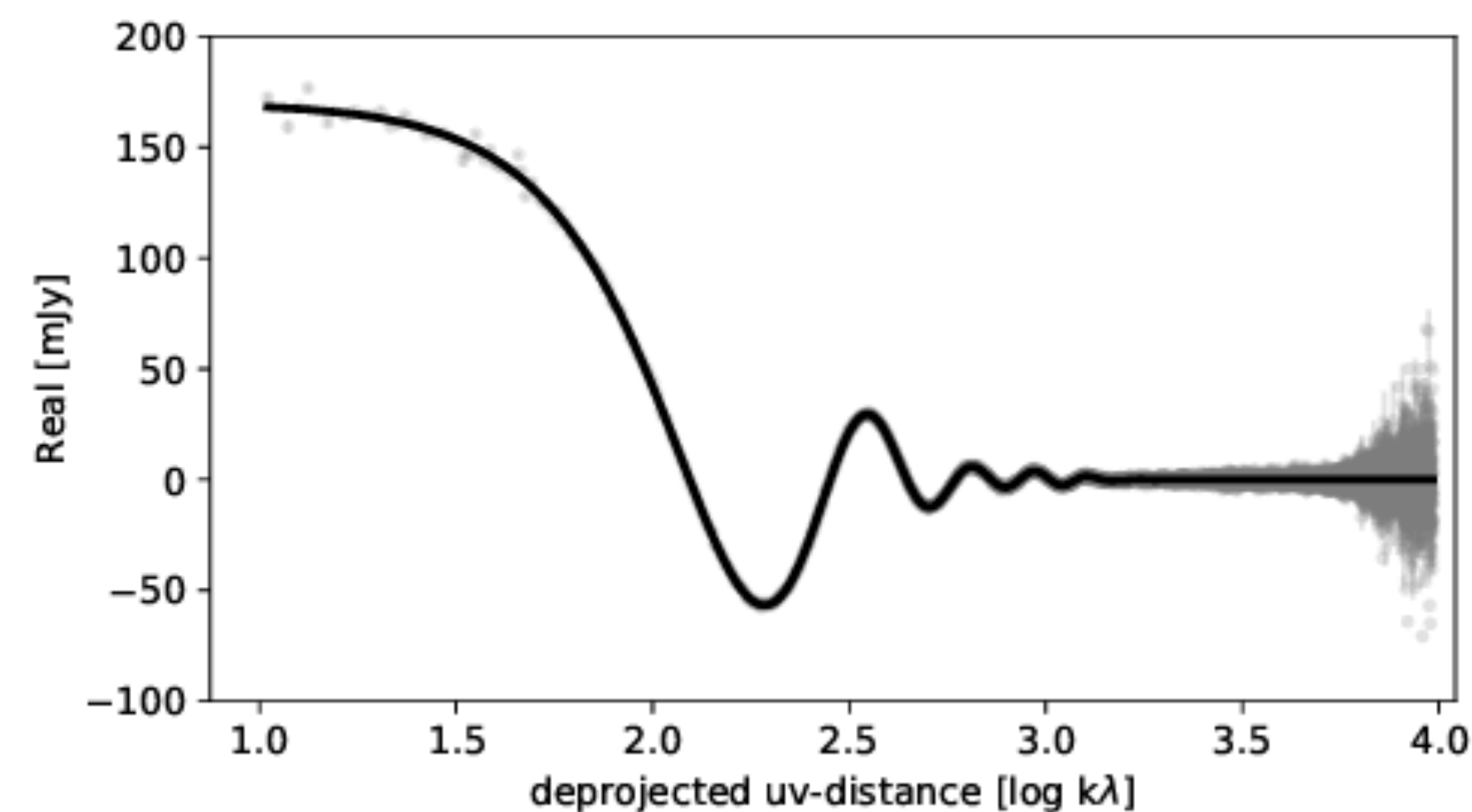
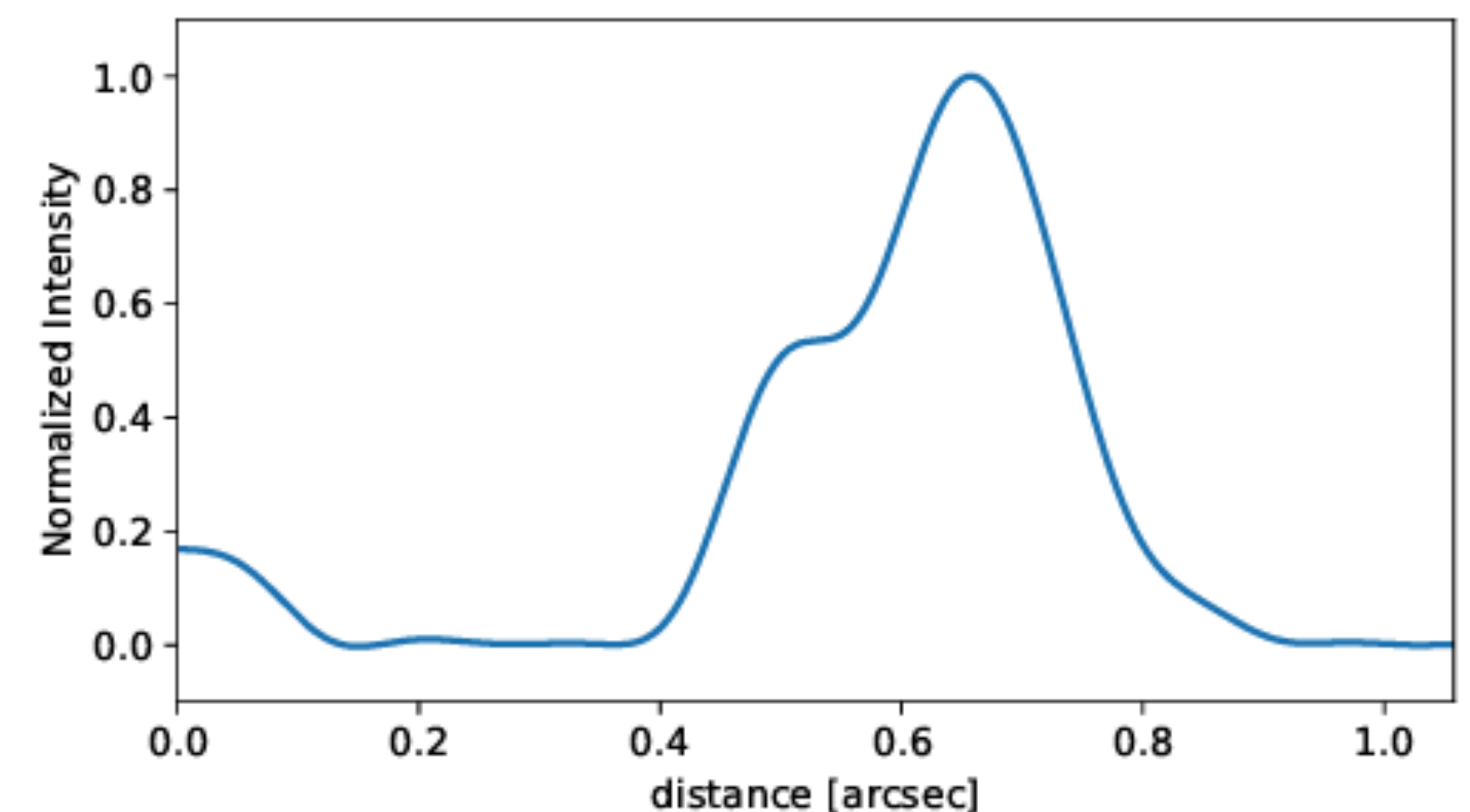
- PDS70 - 低質量星の円盤
 - 2つの原始惑星候補 b,cが検出されている
 - 惑星形成過程&衛星形成にとって重要なサンプル
 - ALMAでも検出されたが感度&解像度不足
- ALMA観測と使用データ



Label	ID	Date	Baselines [m]	Frequency [GHz]	MRS [arcsec]	References
SB16	2015.1.00888.S	2016 Aug 14-18	15-1462	344-355	3.23	Long et al. 2018
IB17	2017.A.00006.S	2017 Dec 2-6	15-6855	346-357	1.05	Keppler et al. 2019; Isella et al. 2019
LB19	2018.A.00030.S	2019 Jul 27-31	92-8547	346-355	0.53	This work



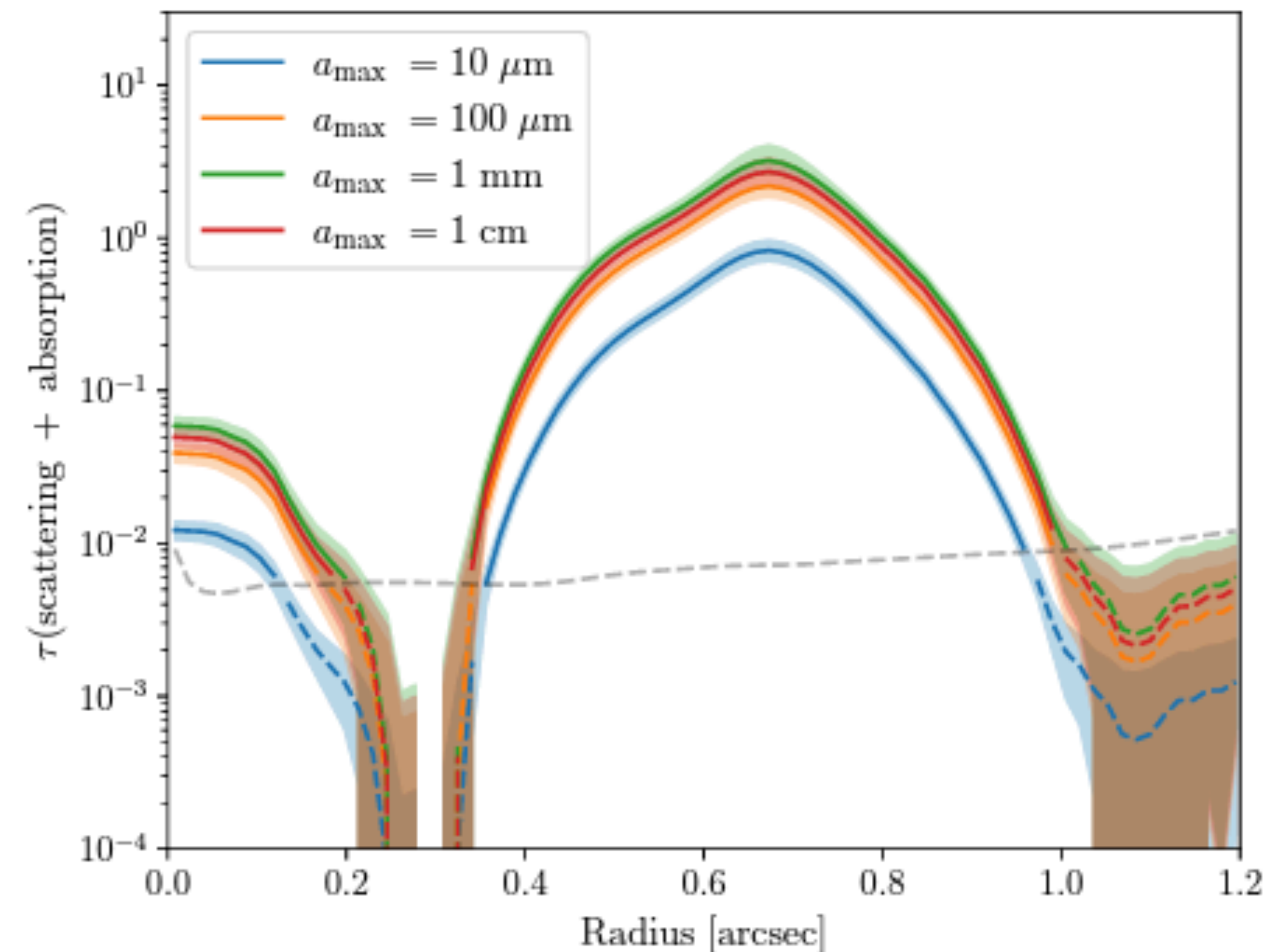
Frankによる動径方向プロファイル



- LB19とIB17でのcsmmの位置変化はエラー以下
→今後の観測が必要

- $70c_{\text{smm}}$ のCPD放射
 - 質量: $0.007 \sim 0.031 M_{\oplus}$ ($a_{\text{max}}: 1 \text{ mm} \sim 1 \mu\text{m}$)
 - 半径: $0.58 \sim 1.2 \text{ au}$ ($\sim 1/3 R_{\text{hill}}$ or $1/10 R_{\text{bondi}}$)
- $70b_{\text{smm}}$
 - 弱い広がった放射でcompact成分はなし
 - $70b$ はずれており関係は不明
 - L5にトラップされたダスト?
 - Dust streamer?
- Outer disk
 - Ring+Shoulderの構造
 - $70c$ のsecondary gap?
 - Unseen planet?

- Inner disk
 - 大ダストか小ダストかは切り分け不可能
 - 赤外超過があるので小ダストはあるはずだが、サブミリ波強度を再現するにはさらに大ダストの存在が必要
 - サブミリは光学的に薄く質量は $0.08\text{--}0.36 M_{\oplus}$



The Substructures in Disks undergoing Vertical Shear Instability: II. Observational Predictions for the Dust Continuum

D.Blanco et al.

High-angular resolution observations at sub-millimeter/millimeter wavelengths of disks surrounding young stars have shown that their morphology is made of azimuthally-symmetric or point-symmetric substructures, in some cases with spiral arms, localized spur- or crescent-shaped features. The majority of theoretical studies with the aim of interpreting the observational results have focused on disk models with planets, under the assumption that the disk substructures are due to the disk-planet interaction. However, so far only in very few cases exoplanets have been detected in these systems. Furthermore, some substructures are expected to appear *before* planets form, as they are necessary to drive the concentration of small solids which can lead to the formation of planetesimals. In this work we present observational predictions from high-resolution 3D radiative hydrodynamical models which follow the evolution of gas and solids in a protoplanetary disk. We focus on substructures in the distribution of millimeter-sized and smaller solid particles produced by the vertical shear instability. We show that their characteristics are compatible with some of the shallow gaps detected in recent observations at sub-mm/mm wavelengths, and present predictions for future observations with better sensitivity and angular resolution with ALMA and a Next Generation Very Large Array.

- VSIに着目した円盤3Dシミュレーションで円盤微細構造を再現
- ALMAやngVLAで特徴的な構造が検出可能かを議論

- Motivation
 - 微細構造を持つ円盤が観測されており、多くが惑星起源で説明されている
 - 一方で、惑星はほぼ検出されていない & 若い円盤でも微細構造が見つかったりしている
 - 観測の円盤微細構造を惑星なしで再現する

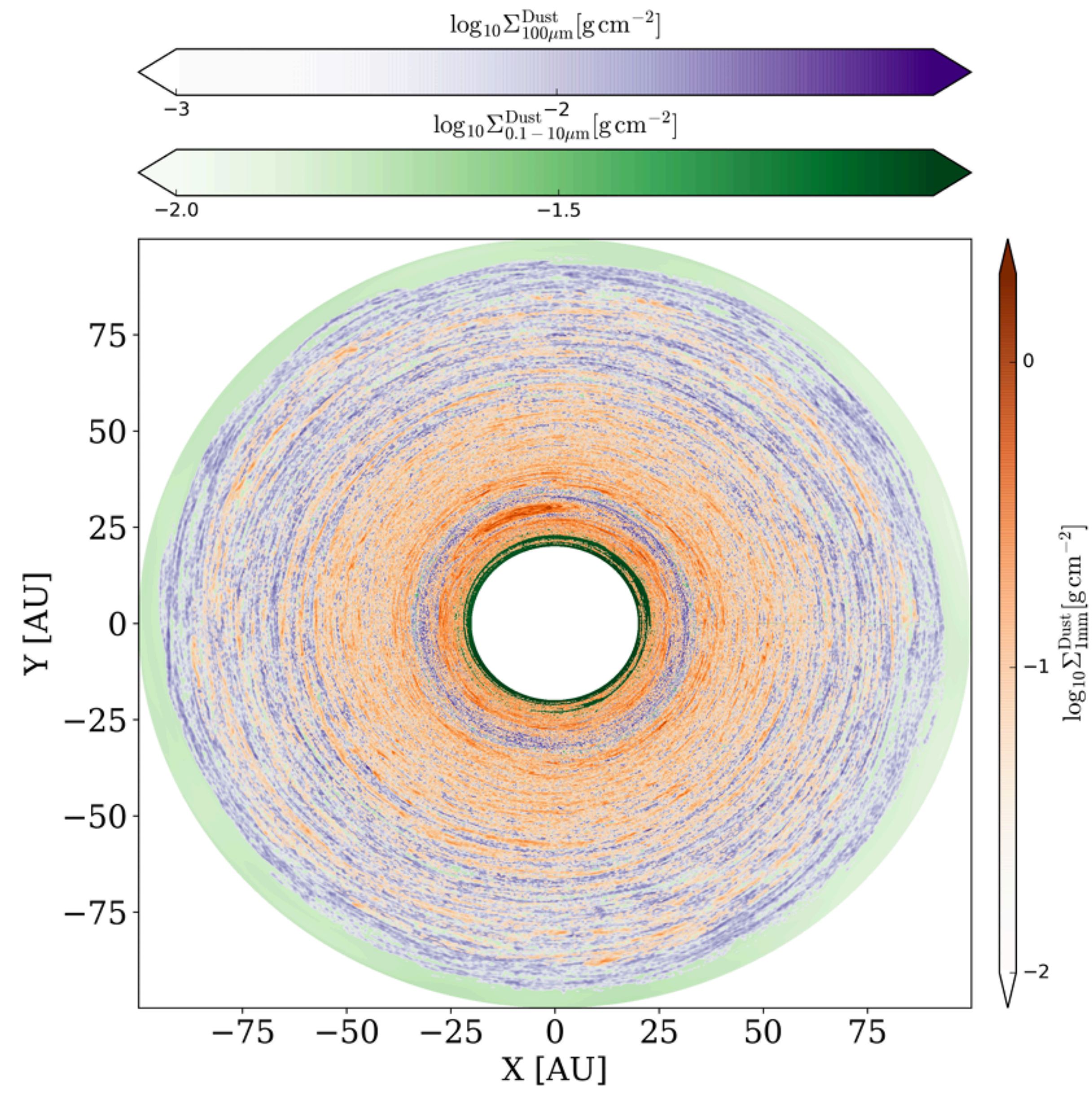
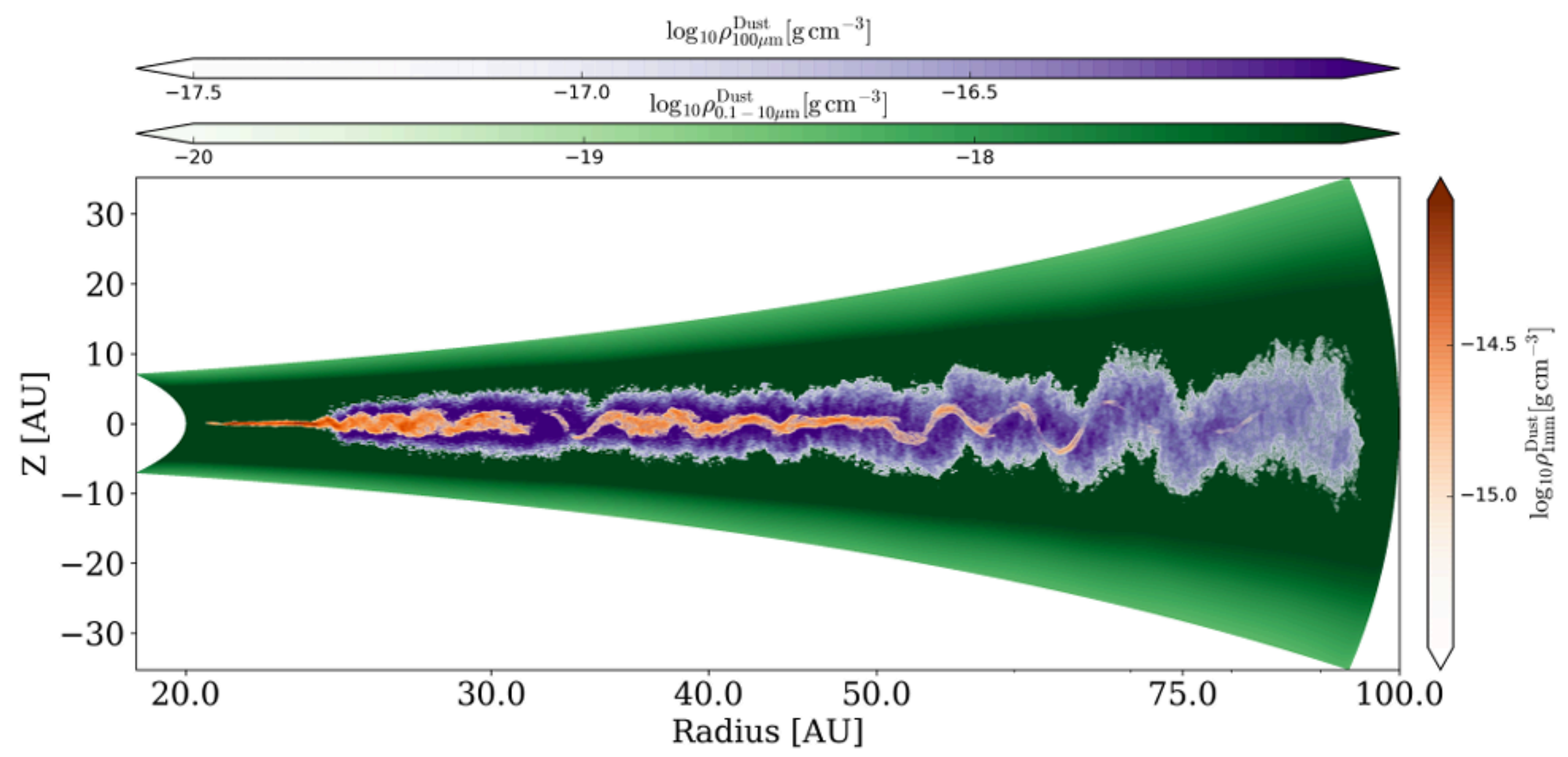
- Flock+17,20と同じ計算で周期増+2pi拡張
 - ダスト入りのhydrodynamic simulation
 - 3つのbinに分けたサイズ分布
 - 円盤全体の微細構造と観測を比較するのに重要
 - 時間進化は次の論文

- RADMCによる放射輸送計算&疑似観測

Surface density	$\Sigma = 6.0 \left(\frac{r}{100\text{AU}}\right)^{-1} \text{ g/cm}^2$
Stellar parameters	$T_{\text{eff},\star} = 4000 \text{ K},$ $R_{\star} = 2.0 R_{\odot}, M_{\star} = 0.5 M_{\odot}$
Opacities	$\kappa_{\star} = 1300 \text{ cm}^2/\text{g}$ $\kappa_{\text{d}} = 400 \text{ cm}^2/\text{g}$
Dust-to-gas ratio	$D2G = 10^{-2}$
Setup	Grid: $r : \theta : \phi$ Domain: $20 - 100 \text{ au} : \pm 0.35 \text{ rad} : 2\pi \text{ rad}$ Resolution: $1024 \times 512 \times 2044$

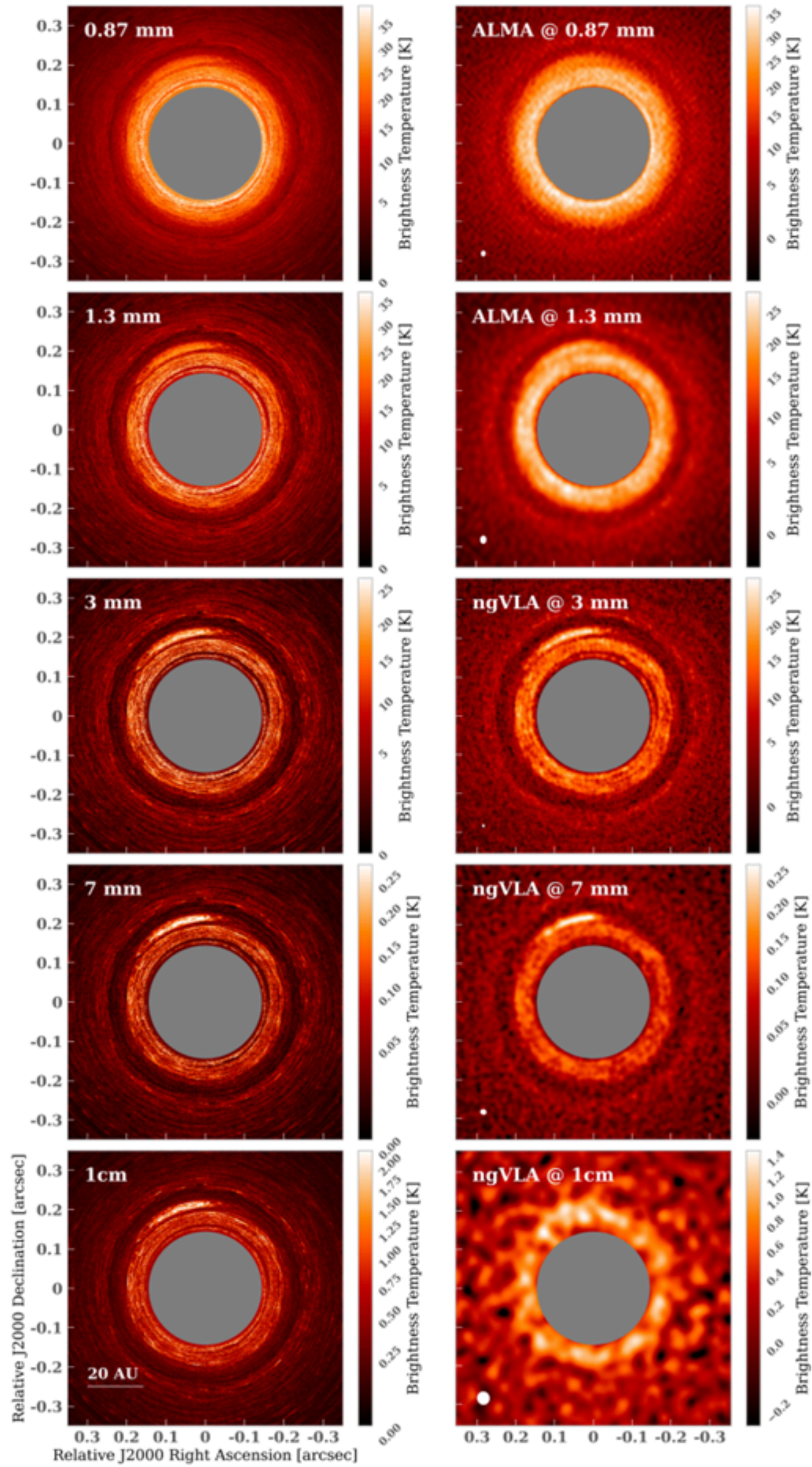
$\lambda \text{ [mm]}$	Dust opacity coefficients [$\text{cm}^2 \text{ g}^{-1}$]					
	Bin 1 (0.1 – 10 μm)		Bin 2 (100 μm)		Bin 3 (1 mm)	
	κ_{abs}	κ_{sca}	κ_{abs}	κ_{sca}	κ_{abs}	κ_{sca}
0.87	4.80	4.09	10.3	35.4	7.79	11.2
1.3	2.15	0.74	3.04	6.07	7.22	12.1
3.0	0.61	0.037	0.66	0.29	4.92	7.99
7.0	0.13	0.00082	0.14	0.0063	0.76	9.82
10.0	0.078	0.00020	0.078	0.0015	0.16	1.84

After 400+400 orbit



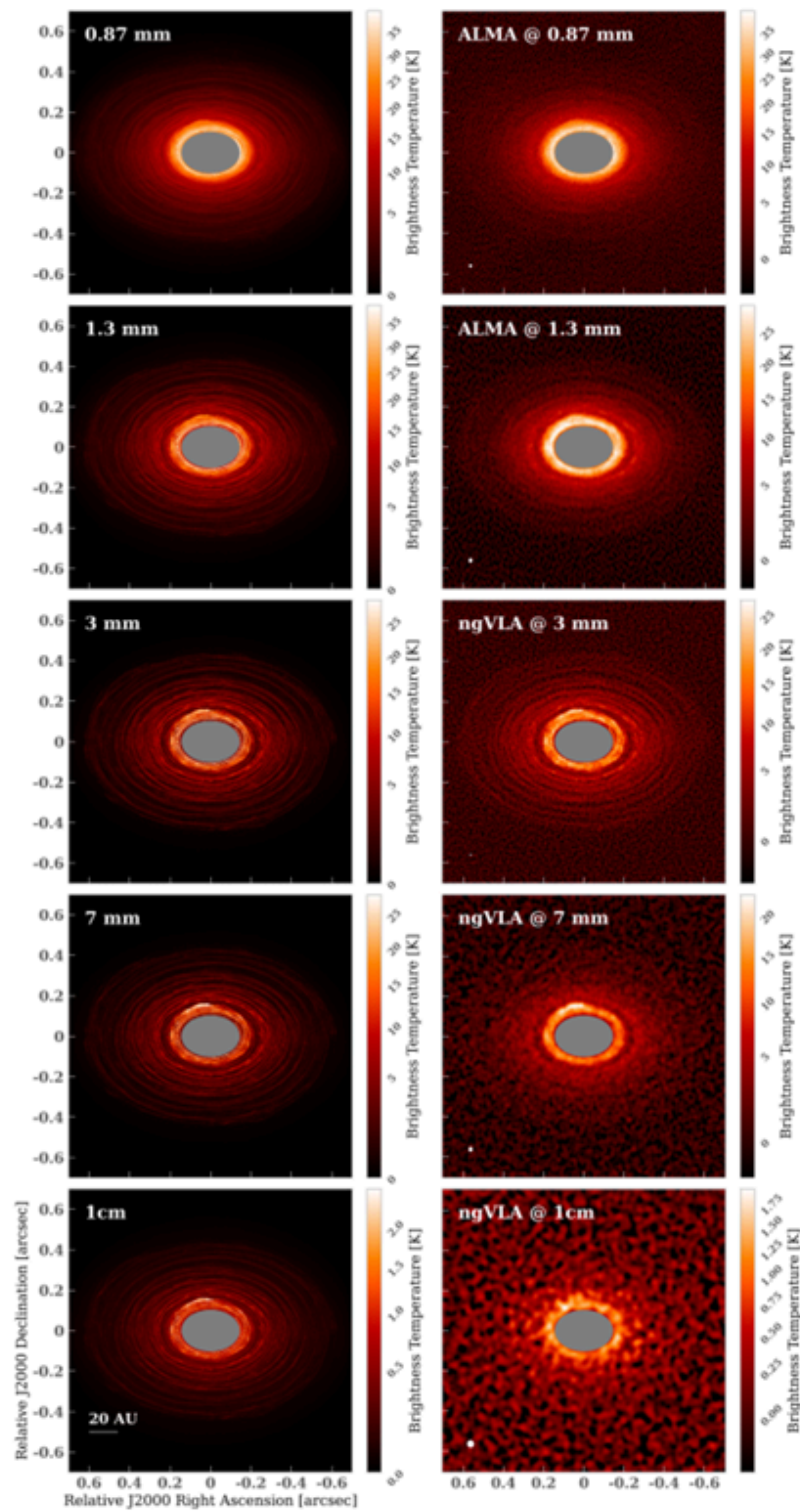
- 140pcの円盤をlongest baselineで疑似観測(~10h)
- Prominent gap
 - Thermal relaxation time (VSI) v.s. radial drift timeで開く
 - 深さや幅は周波数依存
 - ngVLA 3mmでギャップを十分に分解
- Local accumulation
 - 低い周波数で観測可能
 - ngVLA 3mmだと動径方向に分解
- Narrow arcs
 - Gap内側に複数の細いarc構造
 - symmetric構造ではなく arc
 - ngVLA 3mmなら兆候が見える

疑似観測画像パラメータ				
Telescope	λ [mm]	Flux Density [mJy]	Resolution Beam [mas \times mas]	RMS Noise [μ Jy/beam]
ALMA	0.87	450	13 \times 10	12.0
	1.3	150	19 \times 15	6.0
	3	16	44 \times 34	3.9
ngVLA	3	16	8 \times 6	0.34
	7	0.7	14 \times 11	0.085
	10	0.1	34 \times 30	0.10



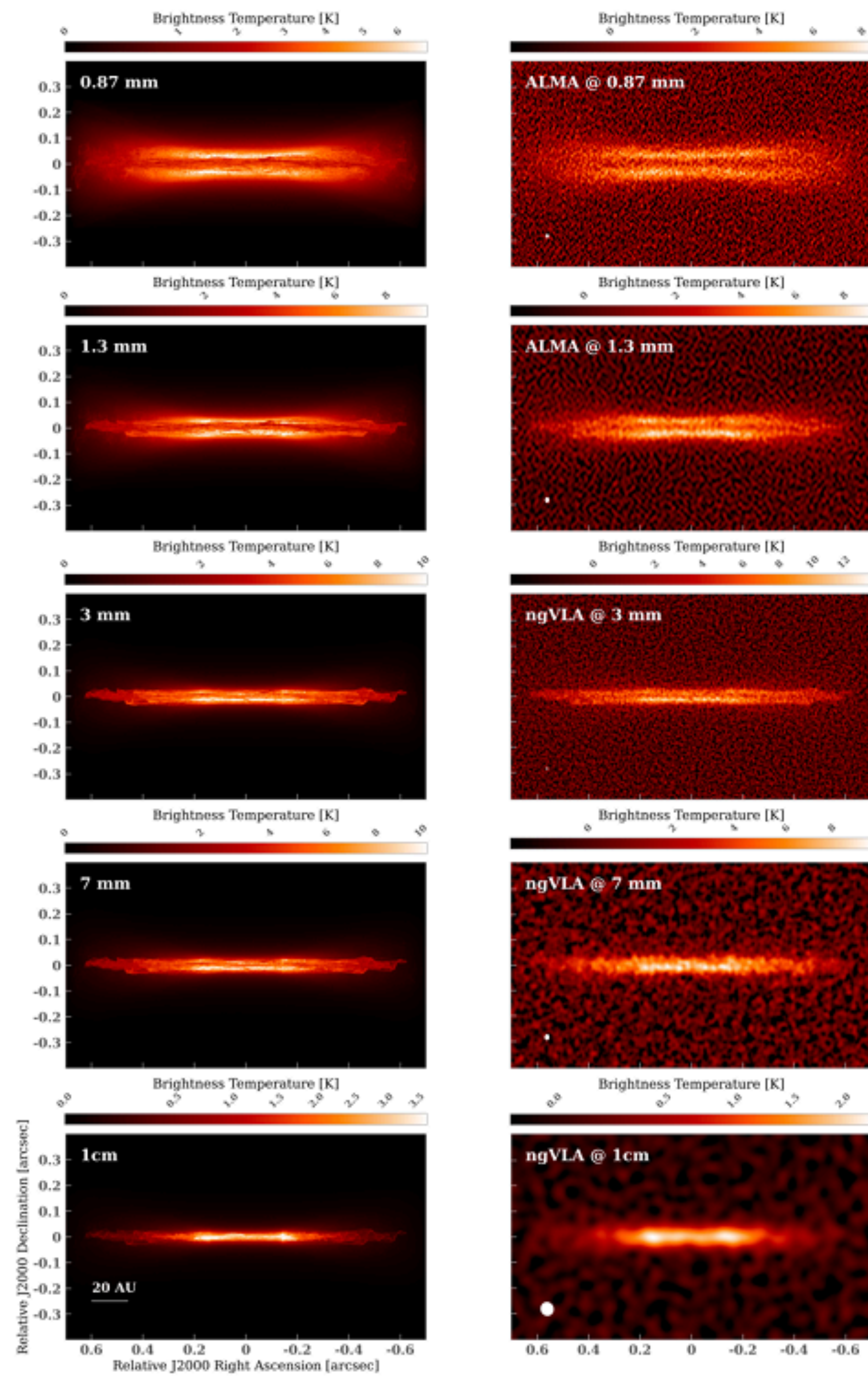
$i=45^\circ$

- inclinationの効果でcontrast↑



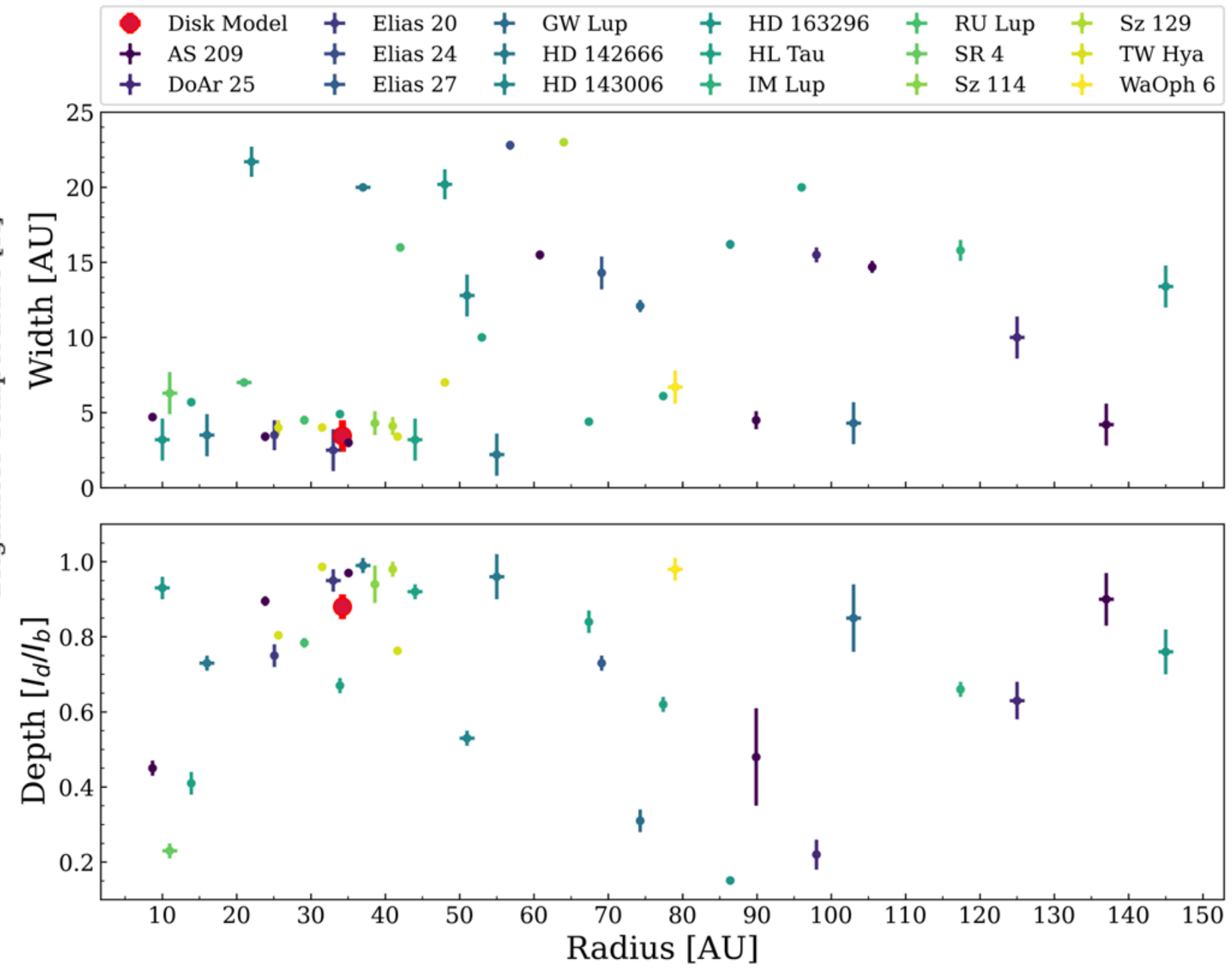
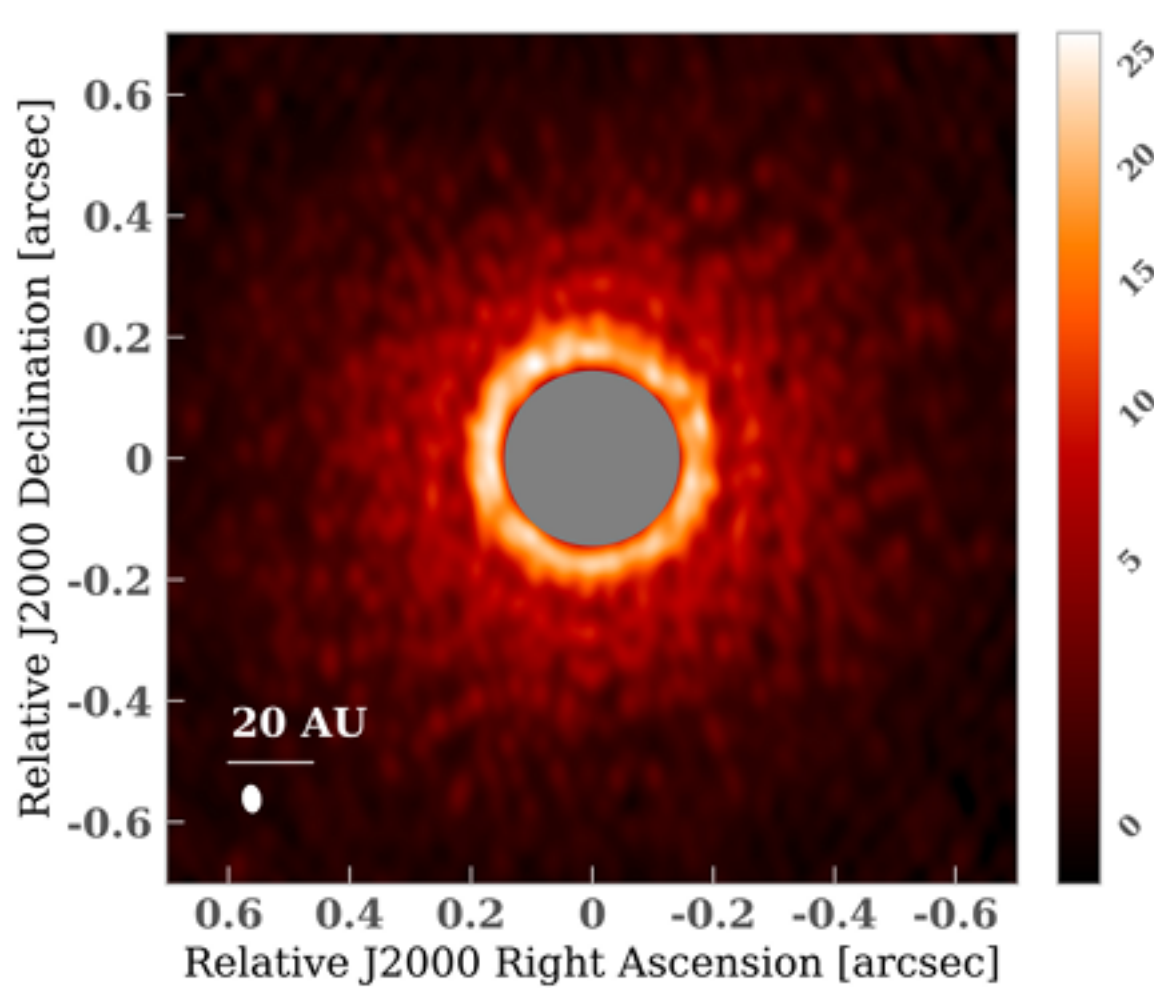
$i=90^\circ$

- $\lambda \uparrow$ でhd \downarrow
- 上下で非対称?
- ngVLA 3mmまで解像できる

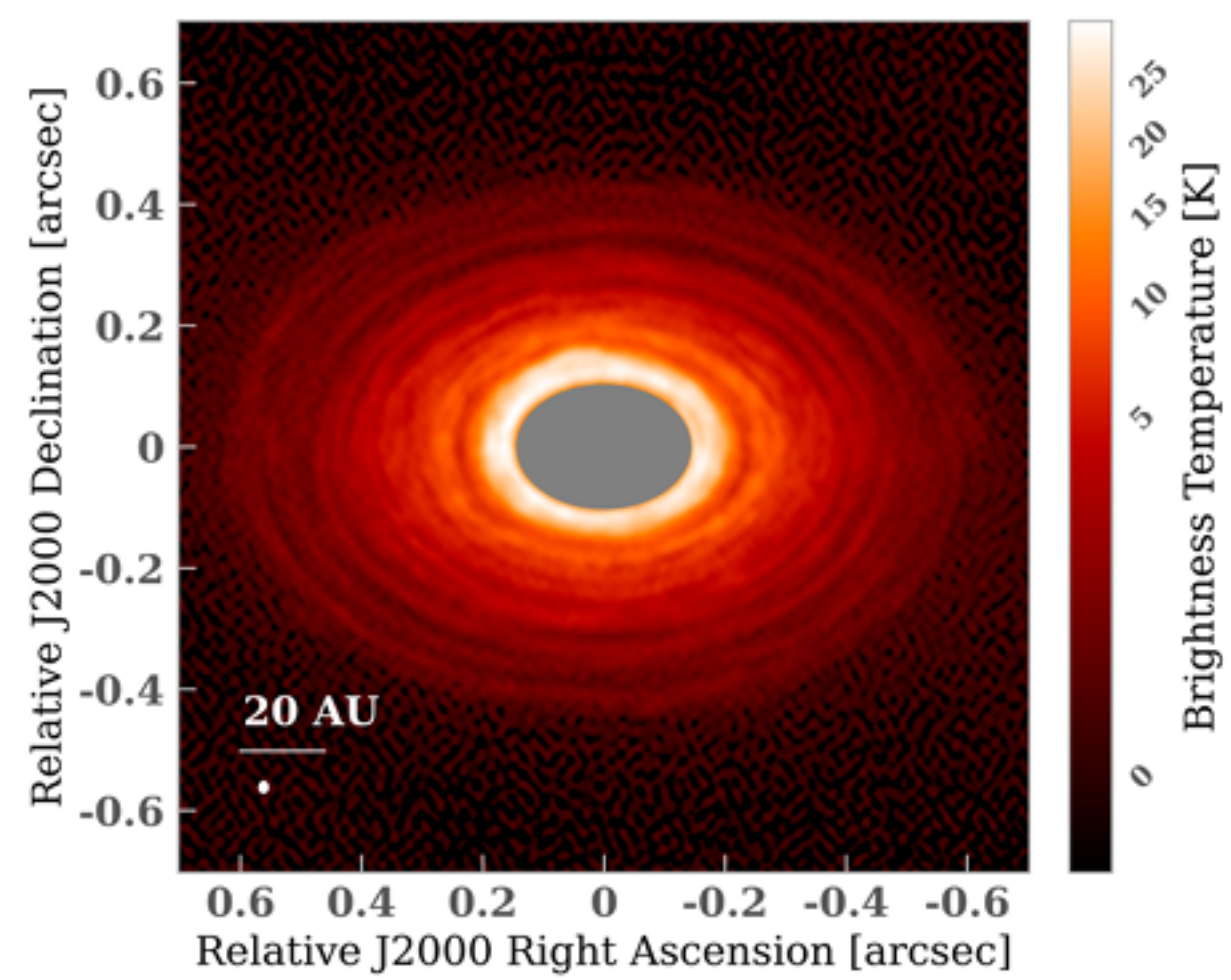


- 観測(DSHARP)との比較
 - 観測はまだ解像度&観測時間不足
- 長基線&長時間積分で構造検出の可能性あり
 - 非軸対象構造やsmall arcs構造
- Observability?
 - モデルの強度: 150mJy at 1.3mm
=>DSHARPやODESIAのサンプルと同程度
- Dust bumpの時間変化検出
 - ngVLA 3mmで3~4週間でproper motionが見えるはず

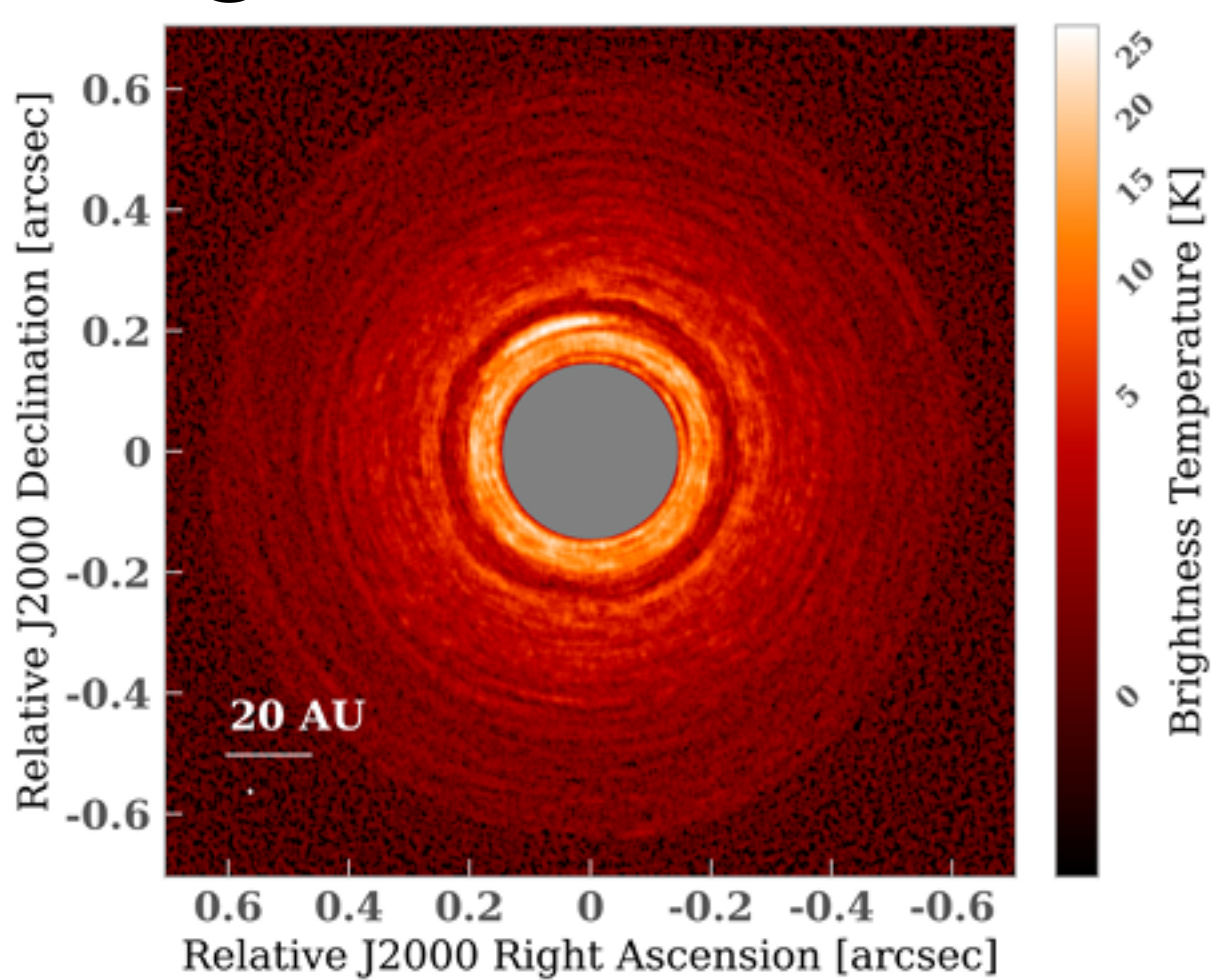
DSHARP設定による疑似観測



ALMA-LB ~40h



ngVLA-LB ~80h



Hourglass Magnetic Field from a Survey of Current Density Profiles

G.Bino et al.

Abstract

Modelling the magnetic field in prestellar cores can serve as a useful tool for studying the initial conditions of star formation. The analytic hourglass model of Ewertowski and Basu (2013) provides a means to fit observed polarimetry measurements and extract useful information. The original model does not specify any radial distribution of the electric current density. Here, we perform a survey of possible centrally-peaked radial distributions of the current density, and numerically derive the full hourglass patterns. Since the vertical distribution is also specified in the original model, we can study the effect of different ratios of vertical to radial scale length on the overall hourglass pattern. Different values of this ratio may correspond to different formation scenarios for prestellar cores. We demonstrate the flexibility of our model and how it can be applied to a variety of magnetic field patterns.

The STAR-MELT Python package for emission line analysis of YSOs

J.Campbell-White et al.

ABSTRACT

We introduce the STAR-MELT Python package that we developed to facilitate the analysis of time-resolved emission line spectroscopy of young stellar objects. STAR-MELT automatically extracts, identifies and fits emission lines. We summarise our analysis methods that utilises the time domain of high-resolution stellar spectra to investigate variability in the line profiles and corresponding emitting regions. This allows us to probe the innermost disc and accretion structures of YSOs. Local temperatures and densities can be determined using Boltzmann statistics, the Saha equation, and the Sobolev large velocity gradient approximation. STAR-MELT allows for new results to be obtained from archival data, as well as facilitating timely analysis of new data as it is obtained. We present the results of applying STAR-MELT to three YSOs, using spectra from UVES, XSHOOTER, FEROS, HARPS, and ESPaDOnS. We demonstrate what can be achieved for data with disparate time sampling, for stars with different inclinations and variability types. For EX Lupi, we confirm the presence of a localised and stable stellar-surface hot spot associated with the footprint of the accretion column. For GQ Lupi A, we find that the maximum infall rate from an accretion column is correlated with lines produced in the lowest temperatures. For CVSO109 we investigate the rapid temporal variability of a redshifted emission wing, indicative of rotating and infalling material in the inner disc. Our results show that STAR-MELT is a useful tool for such analysis, as well as other applications for emission lines.

Core mass function of a single giant molecular cloud complex with $\sim 10^4$ cores

Y.Cao et al.

Similarity in shape between the initial mass function (IMF) and the core mass functions (CMFs) in star-forming regions prompts the idea that the IMF originates from the CMF through a self-similar core-to-star mass mapping process. To accurately determine the shape of the CMF, we create a sample of 8,431 cores with the dust continuum maps of the Cygnus X giant molecular cloud complex, and design a procedure for deriving the CMF considering the mass uncertainty, binning uncertainty, sample incompleteness, and the statistical errors. The resultant CMF coincides well with the IMF for core masses from a few M_{\odot} to the highest masses of $1300 M_{\odot}$ with a power-law of $dN/dM \propto M^{-2.30 \pm 0.04}$, but does not present an obvious flattened turnover in the low-mass range as the IMF does. More detailed inspection reveals that the slope of the CMF steepens with increasing mass. Given the numerous high-mass star-forming activities of Cygnus X, this is in stark contrast with the existing top-heavy CMFs found in high-mass star-forming clumps. We also find that the similarity between the IMF and the mass function of cloud structures is not unique at core scales, but can be seen for cloud structures of up to several pc scales. Finally, our SMA observations toward a subset of the cores do not present evidence for the self-similar mapping. The latter two results indicate that the shape of the IMF may not be directly inherited from the CMF.

The GUAPOS project II. A comprehensive study of peptide-like bond molecules

L.Colzi et al.

Context. Peptide-like molecules, which can take part to the formation of proteins in a primitive Earth environment, have been detected up to now only towards a few hot cores and hot corinos.

Aims. We present a study of HNCN, HC(O)NH₂, CH₃NCO, CH₃C(O)NH₂, CH₃NHCHO, CH₃CH₂NCO, NH₂C(O)NH₂, NH₂C(O)CN, and HOCH₂C(O)NH₂ towards the hot core G31.41+0.31. The aim of this work is to study these species together to allow a consistent study among them.

Methods. We have used the spectrum obtained from the ALMA 3mm spectral survey GUAPOS, with a spectral resolution of ~ 0.488 MHz ($\sim 1.3\text{--}1.7$ km s⁻¹) and an angular resolution of $1''.2 \times 1''.2$ (~ 4500 au), to derive column densities of all the molecular species presented in this work, together with $0''.2 \times 0''.2$ (~ 750 au) ALMA observations from another project to study the morphology of HNCN, HC(O)NH₂ and CH₃C(O)NH₂.

Results. We have detected HNCN, HC(O)NH₂, CH₃NCO, CH₃C(O)NH₂, and CH₃NHCHO, but no CH₃CH₂NCO, NH₂C(O)NH₂, NH₂C(O)CN, and HOCH₂C(O)NH₂. This is the first time that these molecules have been detected all together outside the Galactic center. We have obtained molecular fractional abundances with respect to H₂ from 10^{-7} down to a few 10^{-9} and abundances with respect to CH₃OH from 10^{-3} to $\sim 4 \times 10^{-2}$, and their emission is found to be compact ($\sim 2''$, i.e. ~ 7500 au). From the comparison with other sources, we find that regions in an earlier stage of evolution, such as pre-stellar cores, show abundances at least two orders of magnitude lower than those in hot cores, hot corinos or shocked regions. Moreover, molecular abundance ratios towards different sources are found to be consistent between them within ~ 1 order of magnitude, regardless of the physical properties (e.g. different masses and luminosities), or the source position throughout the Galaxy. Correlations have also been found between HNCN and HC(O)NH₂, and CH₃NCO and HNCN abundances, and for the first time between CH₃NCO and HC(O)NH₂, CH₃C(O)NH₂ and HNCN, and CH₃C(O)NH₂ and HC(O)NH₂ abundances. These results suggest that all these species are formed on grain surfaces in early evolutionary stages of molecular clouds, and that they are subsequently released back to the gas-phase through thermal desorption or shock-triggered desorption.